

## Dynamics of Photoinduced Charge-Density-Wave to Metal Phase Transition in $K_{0.3}MoO_3$

A. Tomeljak,<sup>1,2</sup> H. Schäfer,<sup>1</sup> D. Städter,<sup>1</sup> M. Beyer,<sup>1</sup> K. Biljakovic,<sup>3</sup> and J. Demsar<sup>1,2</sup>

<sup>1</sup>*Physics Department and Center for Applied Photonics, Universität Konstanz, D-78457, Germany*

<sup>2</sup>*Complex Matter Department, Jozef Stefan Institute, SI-1000, Ljubljana, Slovenia*

<sup>3</sup>*Institute of Physics, Zagreb, Croatia*

(Received 21 October 2008; published 13 February 2009)

We present the first systematic studies of the photoinduced phase transition from the ground charge density wave (CDW) state to the normal metallic state in the prototype quasi-1D CDW system  $K_{0.3}MoO_3$ . Ultrafast nonthermal CDW melting is achieved at the absorbed energy density that corresponds to the electronic energy difference between the metallic and CDW states. The results imply that on the subpicosecond time scale when melting and subsequent initial recovery of the electronic order takes place the lattice remains unperturbed.

DOI: [10.1103/PhysRevLett.102.066404](https://doi.org/10.1103/PhysRevLett.102.066404)

PACS numbers: 71.45.Lr, 72.15.Nj, 78.47.J-

In superconductors (SC), it has been known for decades that an intense laser pulse can nonthermally destroy the SC ground state [1]. The energy required to destroy SC should, in the case when all absorbed optical energy is kept in the electronic subsystem during the process of SC suppression, be equal to the condensation energy (energy difference between the free energy of the SC and normal states at  $T = 0$  K). In recent experiments on  $MgB_2$  [2] and the high- $T_c$  SC  $La_{2-x}Sr_xCu_2O_4$  [3] it has been shown, however, that the absorbed optical energy required to suppress SC is substantially higher than the thermodynamically measured condensation energy [3]. This discrepancy was accounted for by considering in detail all energy relaxation pathways on the time scale when SC suppression is achieved. From this analysis it follows that on this time scale a quasiequilibrium between the density of quasiparticles and high frequency phonons is achieved with most of the absorbed energy density being stored in the phonon subsystem [2,3].

Charge density wave systems present another broken symmetry ground state. Here upon cooling through the CDW transition temperature the translational symmetry is broken [4]. The appearance of the long-range CDW is accompanied by the appearance of the gap in the single particle excitation spectrum at the Fermi level, while the collective excitations of the CDW state are the so called amplitude (AM) and phase mode [4]. While real-time studies of photoexcited quasiparticle and collective mode dynamics in CDW compounds have been quite extensive in the weak and moderate perturbation regime [5–9], systematic studies in the high perturbation regime, where the energy of the optical excitation pulse is enough to drive the phase transition from the CDW ground state to the normal metallic state [10,11] are still lacking.

In this Letter we report on the first systematic study of carrier and collective mode dynamics in a prototype quasi-1 dimensional CDW  $K_{0.3}MoO_3$ . Systematic temperature and excitation density dependent measurements of the photoinduced (PI) reflectivity changes reveal that the phase

transition from the ground CDW state to the normal metallic state can be achieved on the femtosecond time scale. From the energy conservation law it follows that the phase transition is nonthermal in origin; i.e., the phase transition is not a result of a simple heating of the sample to above the critical temperature. The absorbed energy density required to optically induce the phase transition is found to be comparable to the electronic energy difference upon CDW condensation. These results give new insight in the ultrafast processes governing the relaxation dynamics in low-dimensional CDW systems. In particular, the results suggest that on the time scale shorter than the period of the characteristic lattice vibrations ( $\approx 0.6$  ps in  $K_{0.3}MoO_3$ , which is the inverse frequency of the AM [5,12]) the charge density modulation is suppressed while the lattice remains unperturbed keeping the  $2k_F$  modulation.

We studied the excitation intensity and temperature dependence of the PI reflectivity dynamics in single crystals of blue bronze  $K_{0.3}MoO_3$  using a degenerate optical pump-probe technique. We used a commercial Ti:sapphire amplifier producing  $6 \mu J$ , 50 fs laser pulses at  $\lambda = 800$  nm (photon energy of 1.55 eV) at a variable repetition rate between 9 and 250 kHz. The laser was used as a source of both excitation and probe pulses. Samples were mounted in an optical helium flow cryostat, with both excitation and probe beam entering the sample at near normal incidence. Because of the strong anisotropy of the induced changes in reflectivity with respect to light polarization [5], the probe laser beam was polarized along the chain [010] direction, while the excitation beam was polarized along the perpendicular [102] direction [4]. To ensure a homogeneous excitation profile, the diameter of the pump beam at the sample position was twice the diameter of the probe beam. To determine the photoexcitation density at the position of the sample with high precision we used a beam profiler. We fitted the beam profile with a Gaussian, and the excitation fluences,  $F$ , used throughout the Letter correspond to the maximum fluence at the center of the beam. Low thermal

conductivity in  $K_{0.3}MoO_3$  [13] can lead to a pronounced increase of the equilibrium temperature in the probed volume, proportional to the average laser power. Therefore, the high excitation experiments were performed at a low repetition rate (10–30 kHz), where at  $F = 1 \text{ mJ/cm}^2$  the temperature increase is  $\leq 10 \text{ K}$ .

Figure 1 presents the induced reflectivity transients taken at 4 K at several excitation densities. At low excitation densities the data show the same behavior as previously reported [5]. The decay dynamics of the (incoherent) electronic response show a biexponential decay with time scales  $\tau_1 \approx 0.3 \text{ ps}$  and  $\tau_2 \approx 7 \text{ ps}$ . The former one, showing critical slowing down upon approaching  $T_c^{3D}$ , was attributed to the recovery of the CDW gap, while the second one was initially tentatively attributed to an overdamped phase mode [5]. Recent detailed studies of the dynamics as a function of  $F$  and applied external electric field however suggest that this longer time scale more likely presents the second stage of the CDW recovery [14]. On top of the incoherent transient an oscillatory (coherent) signal is observed whose Fourier transform, obtained by fast Fourier transform (FFT) analysis, shows several frequency components which can be attributed to the coherently excited AM (the strongest mode at 1.68 THz) and several other phonon modes [5,10,14].

While the PI transient is linear in  $F$  over several orders of magnitude [14], we observe pronounced changes upon increasing the excitation intensity into the  $100 \mu\text{J/cm}^2$  range. The electronic component shows clear saturation at  $F \approx 200 \mu\text{J/cm}^2$  with a maximum induced change in

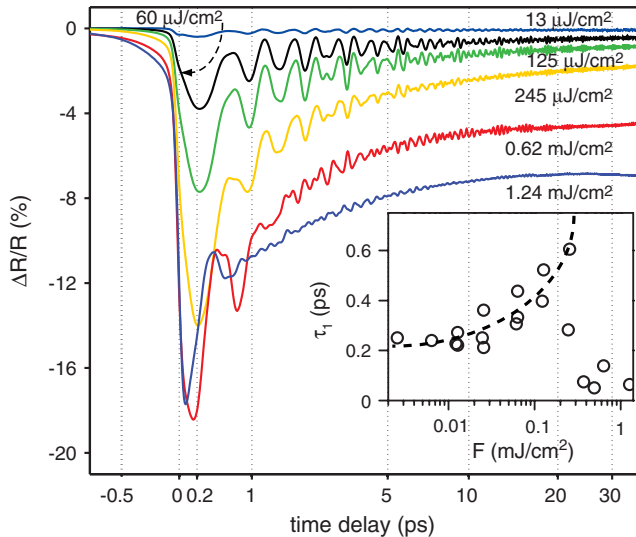


FIG. 1 (color online). PI reflectivity changes in  $K_{0.3}MoO_3$  at 4 K following photoexcitation with 50 fs optical pulses at different excitation fluences [22]. Inset: the  $F$  dependence of the initial decay time  $\tau_1$  determined by fitting the data as described in Ref. [14].  $\tau_1(F)$  displays critical behavior near the threshold fluence of  $\approx 200 \mu\text{J/cm}^2$  (dashed line is a guide to the eye).

reflectivity approaching 18% [15]. One is tempted to ascribe this saturation behavior in reflectivity change to the PI suppression of the CDW order, where this difference in reflectivity corresponds to the change in reflectivity between the normal metallic and the CDW state. Since no measurement of the temperature dependence of reflectivity at optical frequencies is reported to date, we have performed thermomodulation measurements to determine the magnitude and sign of change in equilibrium reflectivity upon increasing the temperature to above  $T_c^{3D}$ . We measured the reflectivity difference between CDW and metallic state at 1.55 eV (800 nm) by heating the sample to above the phase transition using a CW laser. The data show that the reflectivity at 800 nm indeed decreases upon increasing the temperature. The change in reflectivity of  $\sim 10\%$  was observed upon heating from 160 K to just above  $T_c^{3D}$ . At temperatures above  $T_c^{3D}$  the corresponding change in equilibrium reflectivity was less than 1%. Therefore the observed reflectivity change and its saturation behavior upon increasing the excitation fluence are consistent with the PI CDW-M phase transition.

From the rise-time of the reflectivity transient it also follows that this transition happens on the 100 fs time scale after photoexcitation (rise-time is becoming shorter upon increasing  $F$ ). The initial decay time,  $\tau_1$ , shows a pronounced increase near the threshold fluence, followed by a rapid drop as shown in inset to Fig. 1 (the secondary decay time  $\tau_2$  shows only a slight decrease upon increasing  $F$ ). This critical slowing down of relaxation below the threshold for the CDW melting shows similar behavior as in the weak perturbation limit upon increasing the temperature towards  $T_c^{3D}$  [5].

Additional support to the assignment of the saturation behavior to the PI CDW-M transition comes from the study of the oscillatory response, shown in Fig. 2. Here clear suppression of the AM, which presents a fingerprint of the CDW state, is observed at comparable fluences. Figure 2 shows the two-dimensional surface plot of the FFT spectrum of the oscillatory signal as a function of excitation intensity over several orders of magnitude. Several sharp lines are observed, the strongest being that of the AM at about 1.68 THz ( $56 \text{ cm}^{-1}$ ). The two second strongest modes at 2.25 THz ( $74 \text{ cm}^{-1}$ ) and 2.55 THz ( $85 \text{ cm}^{-1}$ ) correspond to zone-folding modes [16,17]. Several weaker phonons in the 3–5 THz range are also observed as in Raman [16], as well as the weak side modes [18] in the vicinity of the AM and the two zone-folding modes.

While Fig. 2 clearly shows strong suppression and increased damping of the AM above  $F \approx 200 \mu\text{J/cm}^2$ , suppression of other phonons follow at the excitation densities that are about 1 order of magnitude higher in  $F$ . More information about the nature of the PI CDW-M phase transition can be gained by looking at the evolution of the FFT spectrum with time at different  $F$ , which is presented in Fig. 3 for four different fluences. Here one clearly

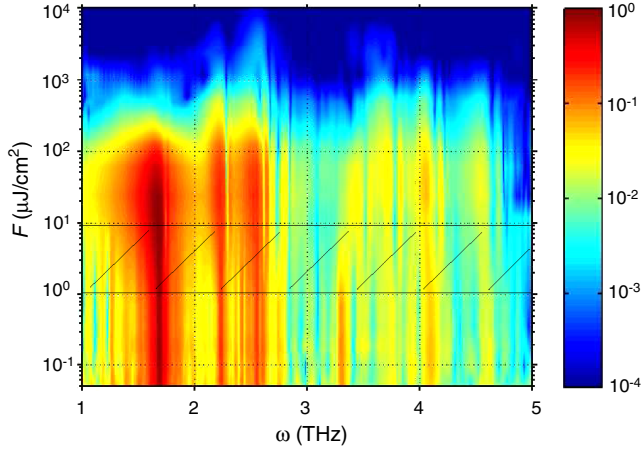


FIG. 2 (color online).  $F$  dependence of the Fourier transform of the oscillatory signal at 4 K. The data were, prior to FFT analysis (time window of 50 ps), normalized to  $F$  for clarity. The area between 1.1 and 9  $\mu\text{J}/\text{cm}^2$  is obtained by interpolation between the low  $F$  data recorded with the Ti:sapphire oscillator and the data recorded with the amplified system. Color coding represents the FFT amplitude. Strong suppression of the AM ( $\approx 1.68$  THz) is observed at  $F \approx 200$   $\mu\text{J}/\text{cm}^2$ , while the other modes vanish at fluences that are about 1 order of magnitude higher.

sees that the AM vanishes at  $F \geq 300$   $\mu\text{J}/\text{cm}^2$  while the two zone-folding modes persist up to  $F \geq 2.5$   $\text{mJ}/\text{cm}^2$  finally disappearing above  $F \geq 3$   $\text{mJ}/\text{cm}^2$ . The fact that high frequency modes survive above the threshold fluence for the PI CDW-M phase transition suggests that on a short

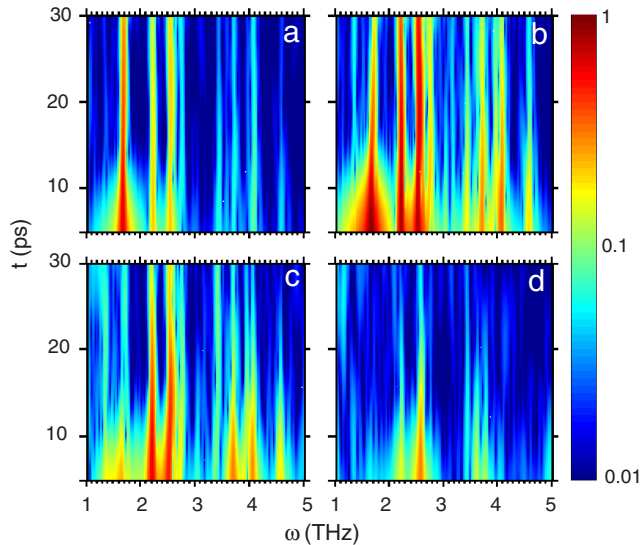


FIG. 3 (color online). The time evolution of the FFT spectrum at 4 K recorded at  $F = 12$   $\mu\text{J}/\text{cm}^2$ , 130  $\mu\text{J}/\text{cm}^2$ , 0.38  $\text{mJ}/\text{cm}^2$ , and 2.5  $\text{mJ}/\text{cm}^2$  [panels (a)–(d)]. The plots are obtained by time-windowed FFT analysis with a 5 ps time window. The AM is strongly suppressed at  $F \geq 200$   $\mu\text{J}/\text{cm}^2$ , while the high frequency modes are present up to  $F \approx 3$   $\text{mJ}/\text{cm}^2$ .

time scale following the PI CDW-M transition and subsequent recovery on the sub-ps time scale (inset to Fig. 1) the lattice remains largely unperturbed. In other words, photoexcitation with a 50 fs optical pulse of  $F > F_{\text{sat}}$  induces melting of the electronic density modulation, which partially recovers on the sub-ps time scale, while the lattice is—on this time scale—uncoupled from the electron subsystem and retains its  $2 k_F$  modulation. Only in the second step of relaxation, which proceeds on the 10 ps time scale, the CDW can be described with a single order parameter where electrons adiabatically follow the lattice.

We studied the  $F$  dependence of the amplitude of the electronic signal at different temperatures below  $T_c^{3D}$  (Fig. 4). Upon increasing the temperature saturation appears at decreasing values of  $F$ . In order to determine the temperature dependence of the saturation fluence,  $F_{\text{sat}}$ , we fit the data with the simple saturation model, which is described in detail in Ref. [3]. The temperature dependence of  $F_{\text{sat}}$ , together with the corresponding absorbed energy density per unit cell volume (u.c.v) [19],  $E_{\text{sat}}$ , is presented in Fig. 4(b). To find whether the CDW melting is a result of a simple pulsed heating or is nonthermal in origin we calculated the expected temperature rise  $\Delta T$  which corresponds to  $E_{\text{sat}}$ , using  $E_{\text{sat}} = \int_{T_0}^{T_0+\Delta T} c_p(T) dT$ . Here  $c_p$  is the total specific heat [13]. At  $T_0 = 4$  K and  $E_{\text{sat}} \approx 60$   $\text{meV}/\text{u.c.v.}$  we obtain  $\Delta T \lesssim 40$  K, while at higher  $T_0$  this value is considerably smaller ( $\Delta T \lesssim 3$  K at 172 K and  $E_{\text{sat}} \approx 20$   $\text{meV}/\text{u.c.v.}$ ). In fact, the absorbed energy density required to heat  $\text{K}_{0.3}\text{MoO}_3$  from 4 K to its phase transition  $T_c^{3D} = 183$  K is about 600  $\text{meV}/\text{u.c.v.}$ , an order of magnitude higher than  $E_{\text{sat}}$ . It follows that the PI CDW-M phase transition is nonthermally driven.

Observation of coherently excited zone-folded modes at fluences up to 1 order of magnitude higher than  $F_{\text{sat}}$

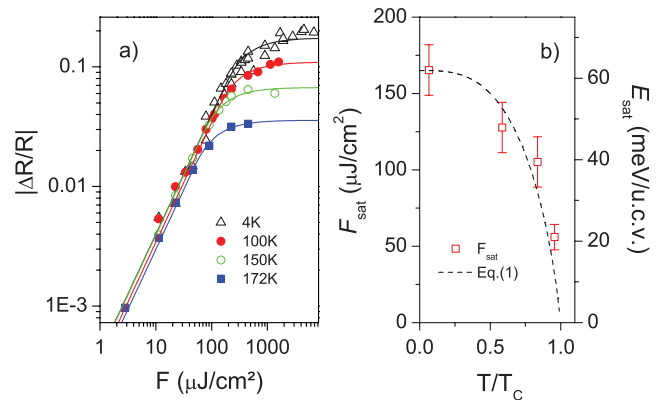


FIG. 4 (color online). (a)  $F$  dependence of the PI reflectivity maximum at several temperatures below  $T_c^{3D}$ . The solid lines are fits with the simple saturations model [3]. (b) Saturation fluences extracted from (a) and the corresponding absorbed energy densities in  $\text{meV}$  per unit cell volume. The dashed line represents the calculated  $T$  dependence of  $E_{\text{el}}$  given by Eq. (1), where BCS  $T$  dependence of  $\Delta$  was used.



suggests, that on the sub-ps time scale after photoexcitation, the electrons are nearly uncoupled from the lattice. In this case  $E_{\text{sat}}$  should be compared to the energy gain of the electronic subsystem upon CDW condensation,  $E_{\text{el}}$ . To estimate  $E_{\text{el}}$  we used the mean-field expression in the weak coupling limit, given by Eq. 3.40 in Ref. [4]:

$$E_{\text{el}} = -n(\epsilon_F)\Delta^2\left(\frac{1}{2} + \log\frac{2\epsilon_F}{\Delta}\right). \quad (1)$$

Here  $n(\epsilon_F)$  is the normal state density of states at the Fermi energy,  $\epsilon_F$ , and  $\Delta$  is the value of the CDW gap. Using  $\Delta = 60$  meV,  $\epsilon_F = 0.24\text{--}0.39$  eV and  $n(\epsilon_F) = 4\text{--}6$  eV<sup>-1</sup>/u.c.v. [4,21] we obtain  $E_{\text{el}}(4\text{ K}) = 37\text{--}66$  meV/u.c.v.. This value is in excellent agreement with  $E_{\text{sat}}(4\text{ K}) \approx 60$  meV/u.c.v., giving further support to the argument that during PI CDW melting the electronic order parameter is decoupled from the lattice on the sub-ps time scale. At  $F \gtrsim 3$  mJ/cm<sup>2</sup>, which corresponds to the absorbed energy density of 1 eV/u.c.v., other modes are also completely suppressed. This energy density is in good agreement with the calculated energy density required to heat up the excited volume to above  $T_c^{3D}$ . In this regime, recovery proceeds on a much longer time scale which is determined by heat diffusion out of the excited volume. The temperature dependence of  $E_{\text{sat}}$ , shown in Fig. 4(b), shows good agreement with the expected  $T$  dependence of  $E_{\text{el}}$ . The dashed line in Fig. 4(b) shows  $E_{\text{el}}(T)$  calculated from Eq. (1), where the BCS  $T$  dependence of  $\Delta$  was used [4].

We have shown that in K<sub>0.3</sub>MoO<sub>3</sub> the PI CDW-M phase transition is nonthermal and takes place on the 100 fs time scale. The good agreement between measured  $E_{\text{sat}}$  and calculated  $E_{\text{el}}$ , the observation of the order parameter recovery on the sub-ps time scale, and the observation of zone-folded phonons high above  $E_{\text{sat}}$  suggest that during the process of melting and sub-ps recovery of the electronic modulation the lattice remains nearly frozen. This has an important implication for understanding the ultrafast relaxation processes in systems with reduced dimensionality, in particular, for the systems with strong electron-phonon interactions that lead to phenomena like charge density modulation. The initial reconstruction of the CDW state is found in all systems studied thus far to proceed on the sub-ps time scale [5–11]. Importantly, this time scale is one to two orders of magnitude faster than in the high- $T_c$  superconductors [3], and is indeed close to the typical time scale for electron-phonon thermalization. The formation of the CDW requires freezing of a phonon and our results do imply that the lattice remains frozen in its modulated state on the sub-ps time scale after perturbation. Therefore, the extremely fast order parameter recovery in

this entire class of low-dimensional materials [5–11] could be a consequence of the fact that on the short time scale after photoexcitation the lattice remains in its unperturbed state. Thereby, the retaining  $2k_F$  modulation presents a strong potential well driving ultrafast reformation of the charge density modulation. Clearly, further theoretical studies as well as studies of the ultrafast structural dynamics are required to shed additional light on these fascinating phenomena.

We would like to acknowledge V. V. Kabanov, P. van Loosdrecht, T. Dekorsy, and L. Degiorgi for valuable discussions. This work was supported by Sofja-Kovalevskaja Grant from the Alexander von Humboldt Foundation, Center for Applied Photonics and Zukunfts Kolleg at the University of Konstanz, Croatian MSES project No. 035-0352827-2842 and AdFutura.

- 
- [1] L. R. Testardi, Phys. Rev. B **4**, 2189 (1971).
  - [2] J. Demsar *et al.*, Phys. Rev. Lett. **91**, 267002 (2003); J. Demsar *et al.*, Int. J. Mod. Phys. B **17**, 3675 (2003).
  - [3] P. Kusar *et al.*, Phys. Rev. Lett. **101**, 227001 (2008).
  - [4] G. Grüner, *Density Waves in Solids* (Addison-Wesley, Reading, MA, 1994).
  - [5] J. Demsar *et al.*, Phys. Rev. Lett. **83**, 800 (1999).
  - [6] J. Demsar *et al.*, Phys. Rev. B **66**, 041101 (2002).
  - [7] D. Dvorsek *et al.*, Phys. Rev. B **74**, 085211 (2006).
  - [8] L. Perfetti *et al.*, Phys. Rev. Lett. **97**, 067402 (2006).
  - [9] K. Shimatake, Y. Toda, and S. Tanda, Phys. Rev. B **75**, 115120 (2007).
  - [10] D. M. Sagar *et al.*, J. Phys. Condens. Matter **19**, 346208 (2007).
  - [11] F. Schmitt *et al.*, Science **321**, 1649 (2008).
  - [12] G. Travaglini and P. Wachter, Phys. Rev. B **30**, 1971 (1984).
  - [13] R. S. Kwok and S. E. Brown, Phys. Rev. Lett. **63**, 895 (1989); J. W. Brill *et al.*, *ibid.* **74**, 1182 (1995); Z. Bihari *et al.*, Europhys. Lett. **40**, 73 (1997).
  - [14] A. Tomeljak *et al.*, Physica B (Amsterdam) (2009) (to be published).
  - [15] Similar saturation behavior was observed also in Ref. [10]. There saturation is seen at higher fluences, which can be ascribed to the different experimental configuration used.
  - [16] D. M. Sagar *et al.*, New J. Phys. **10**, 023043 (2008).
  - [17] J. P. Pouget *et al.*, Phys. Rev. B **43**, 8421 (1991).
  - [18] H. Schäfer *et al.* (to be published).
  - [19] Absorbed energy density is calculated using published values [20] of the dielectric constant at 1.55 eV.
  - [20] L. Degiorgi *et al.*, Phys. Rev. B **44**, 7808 (1991).
  - [21] D. C. Johnston, Phys. Rev. Lett. **52**, 2049 (1984).
  - [22] For presentation purposes the  $x$  axis is logarithmic with zero time delay shifted to 1.5 ps prior to logarithmation.